Insights into the properties of surface waters and their associated nanofiltration membrane fouling: the importance of biopolymers and high molecular weight humics

Long Tian [a,b], Peng Zhou [a], Zhaoyang Su [a], Ting Liu [b]*, Nigel Graham [c], Tom Bond [d], Wenzheng Yu [a]*

[a] *State Key Laboratory of Environmental Aquatic Chemistry, Key Laboratory of Drinking Water Science and Technology, Research Center for Eco-Environmental Sciences, Chinese Academy of Sciences, Beijing 100085, People's Republic of China. (wzyu@rcees.ac.cn)*

[b] *School of Chemistry and Chemical Engineering, Beijing Institute of Technology, Beijing 100081, China. (liuting@bit.edu.cn)*

[c] *Department of Civil and Environmental Engineering, Imperial College London, South Kensington Campus, London SW7 2AZ, UK. (n.graham@imperial.ac.uk)*

d Department of Civil and Environmental Engineering, University of Surrey, Guildford, Surrey GU2 7XH, United Kingdom

Abstract

Nanofiltration (NF) membrane fouling by surface waters is still an unclear and unpredictable topic due to the heterogeneity and variability of natural organic matter (NOM) in waters. The objective of this study was to identify the key water quality parameter/s responsible for NF membrane fouling. Six representative surface waters were systematically investigated in terms of the water quality characteristics and their fouling potential on a polyamide NF membrane. The results showed that these waters exhibited significant discrepancies in DOC, Ca^{2+}, composition, and chemical characteristics of NOM. Removal

performance and membrane fouling analysis indicated a preferential rejection of hydrophobic over hydrophilic NOM, and the hydrophobicity of NOM was positively correlated with reversible fouling. The biopolymer content exhibited a strong positive correlation to the total membrane fouling and irreversible fouling, indicating that it could be used as a surrogate of NF fouling behaviors by surface waters. Ca^{2+} and humic substances contents could not explain the membrane fouling due to their insignificant correlation with membrane fouling. However, the proportion of high molecular weight component in humic substances (%-HMW) exhibited a negative correlation with the total membrane fouling and irreversible fouling, suggesting that the HMW component has a positive effect on NF membrane fouling prevention. A reasonable explanation is that the HMW component is preferentially deposited on the membrane surface, forming a 'controlling layer' that prevents low MW organics from entering and blocking the membrane pores.

Keywords: Drinking water treatment; Nanofiltration membrane fouling; Biopolymer; High molecular weight component; Correlation analysis;

1. Introduction

The problems of water scarcity and water pollution threaten the humanity in the 21st century due to the challenges posed by the urbanization, population growth and climate change [1-3]. For example, China, with a population of 1.4 billion and rapidly growing economy is facing a shortfall of 40 billion tonnes of water a year on average, and this deficit is expected to increase with the future national development [4,5]. The gap between the supply and demand of clean water is accelerating the research and development of novel and facile methods to produce clean water. In recent years, the emergence of state-of-the-art membrane technologies (microfiltration-MF [6], ultrafiltration-UF [7], nanofiltration-NF [8], reverse osmosis-RO [9] and forward-osmosis-FO [10]) has been recognized as a new generation of water purification methods. Their advantages include high separation effectiveness, low chemical usage, competitive cost and scalability [3]. Among the various membrane technologies, NF is

considered to be one of the most promising techniques for water purification due to its lower operating pressure than RO, and greater separation efficiency than UF [11]. In practice, NF shows high removal efficiency for most of the organic matter, microorganisms and viruses in water, including pathogens which pose a significant threat to human health [12]. Thus, NF is a promising technology for supplying safe potable water from surface water. However, membrane fouling is the main obstacle restricting the efficiency of membrane processes, since the adsorbed foulant and the cake layer result in a significant increase in energy consumption. Although foulants can be partially removed by physical and chemical backwashing, the frequent cleaning not only complicates the operation, but also reduces the membrane lifetime [13,14]. Therefore, a better understanding about the fouling mechanisms and developing effective approaches to mitigate membrane fouling are urgently required.

Natural organic matter (NOM) is a heterogeneous matrix of organic compounds (mainly composed of proteins, polysaccharides and humic substances) which is ubiquitous in natural water sources [15-17]. Several studies have shown that NOM was the major cause of membrane fouling [18-20]. Typical model substances, such as bovine serum albumin (BSA), sodium alginate (SA) and humic acid (HA) have been widely applied to investigate NOM fouling because they are easy to detect and control [21-23]. For instance, Shim et al. [23] studied NF membrane fouling by different types of organic matter and found that SA caused more fouling than BSA and HA at low operating pressures. Synergistic fouling, such as from HA-BSA and HA-SA mixtures have also been reported in the literature [24]. Further, some studies suggested that hydrophilic NOM fractions (i.e. polysaccharides and proteins) were the major factors increasing permeate resistance, whereas hydrophobic fractions caused less fouling [25,26]. Another study found that the hydrophilic NOM fractions were preferentially deposited on the membrane surface, which decreased the negative zeta potential of the membrane, and subsequently, hydrophobic NOM was more readily deposited on the membrane surface due to the decreased electrostatic repulsion [27]. Meanwhile, the presence of calcium ions (Ca^{2+}) also be considered an important factor affecting the membrane performance. The presence of Ca^{2+} can function as a bridge between negatively charged NOM and the membrane surface, leading

to a denser cake layer which exacerbates membrane fouling [28,29]. A number of other factors, including water chemistry (i.e. pH, zeta potential), membrane characteristics (i.e. surface roughness, charge, hydrophilicity) and operational conditions (i.e. operation pressure, cross-flow or dead-end filtration) have also been reported in previous studies that correlates with membrane fouling [30-33].

To date, many studies focusing on the NF membrane fouling while treating surface waters have been limited to model substances. Although these reagents can represent the NOM in natural surface water, their composition, molecular weight distribution and chemical functionality differ from NOM found in real surface waters [34,35]. Therefore, membranes can exhibit distinct or even opposite performance when exposed to these model substances and surface water NOM [34,36]. Particularly in recent years, membrane fouling by real natural waters have been investigated, with some promising findings [37-39]. However, these studies were typically limited to a small number of water samples and/or NOM characterization techniques. In addition, the complicated extraction process is a major obstacle in separating individual NOM fractions in natural waters and investigating their effects (positive or negative) on NF performance. Moreover, the composition and physicochemical properties of NOM are highly heterogenous and variable, depending on geographical location, hydrological conditions and temporality [40,41]. In this aspect, the universal relationship between specific water quality parameters and NF membrane fouling is still unclear and needs to be further explored.

In light of the aforementioned analysis, this study aimed to provide broadly applicable insights into the fouling potential of NF by surface waters, thus providing a benchmark for the development of strategies to control membrane fouling and boost its sustainability. We investigated the performance and fouling mechanism of a loose NF membrane by separately treating the six surface waters having diverse chemical nature and compositions. Water quality parameters, NOM characteristics and membrane fouling were probed through state-of-the-art experimental techniques. The key factor/s responsible for NF membrane fouling and the relationships between specific water quality parameters and membrane fouling were systematically studied through correlation analysis.

2. Materials and methods

2.1. Source waters

Six water samples from two regions in China, including three water samples from the south (Yiwu reservoir water, Hangzhou water and Yiwu Village water, referred to as YWR, HZ and YWV, respectively. Zhejiang Province China) and three from the north (Miyun reservoir water, South Long River water and Zizhuyuan park water, referred to as JM, NCH and ZZY, respectively. Beijing China) were collected in June 2019 (Figure S1). These waters encompass a range of source water types, including reservoir waters (YWR and JM), river waters (HZ and NCH) and lake waters (YWV and ZZY). Samples were collected and transferred to the laboratory within one day, and then filtered by microfiltration membrane (0.22 μm) to remove microorganisms and particulates before storage at 4 ^{o}C. Before NF filtration experiments, the water samples were restored to room temperature ~25 ^{o}C.

2.2. Water quality and NOM characterization

A suite of analytical methods were utilized to characterize raw water quality and NOM. A commercial pH meter (FE28, METTLER TOLEDO, China), conductivity meter (FD38, METTLER TOLEDO, China), and liquid zeta potential analyzer (ZS90, Malvern, UK) were used to evaluate the pH, conductivity and charge of the water, respectively. Concentrations of metal cations were determined using inductively coupled plasma optical emission spectrometry (ICP-OES, Optima 8300, PerkinElmer, USA). Turbidity was characterized indirectly by a laboratory UV-Vis spectrophotometer (UV-2600, Shimadzu, Japan) based on visible light adsorption at 600 nm (OD 600) [42]. Dissolved organic carbon (DOC) was determined with a total organic carbon (TOC) analyzer (TOC-V_{wp}, Shimadzu, Japan). Molecular size, degree of aromatic ring substitution and aromatic index of organic matters were also characterized by UV-Vis spectrophotometer based on E_{254}/E_{365} (the ratio of UV adsorption at 254 to 365 nm), E_{253}/E_{203} (the ratio of UV adsorption at 253 to 203 nm) and SUVA (the ratio of UV adsorption at 254 to DOC). Attenuated total reflection fourier transform infrared spectroscopy (ATR-FTIR, Spectrum Two, PerkinElmer, USA) was carried out to identify the different functional groups

of NOM (after freeze-drying). FTIR analysis was undertaken at wavenumbers from 400-4000 cm^{-1} in 2 cm^{-1} steps, and then the results were treated by baseline correction and normalization.

Three-dimensional excitation-emission matrix fluorescence spectroscopy (EEM, F-4600, Hitachi, Japan) was employed to identify the fluorescent components (tryptophan-like, tyrosine-like, fulvic acid-like, soluble microbial by-product-like and humic acid-like substances) within NOM. The emission scan range was registered from 200 to 550 nm at 5 nm steps and excitation wavelengths were performed from 200 to 450 nm at 5 nm intervals. The slit widths were fixed to 5 nm and the scanning speed was maintained at 2400 nm/min. A quantitative analysis method, named fluorescence regional integration (FRI) [43], was applied to quantify the proportion of each fluorescent component in the EEM spectrum and the results were used for subsequent correlation analysis.

Size exclusion chromatography (SEC) with UV detection and auto-sampler was used to detect the apparent molecular weight (MW) distribution of organic matters in water. SEC was performed using a Waters HPLC system with a SEC column (Phenomenex, BioSep 5 μm, SEC-s3000, 290A) and Security Guard^{TM} Cartridges (Phenomenex, KJ0-4282). Sodium acetate (10 mM, Aldrich, USA) was the mobile phase, with a flow rate of 1 mL/min. The UV/VIS detector operated at 254 nm and other components of the SEC instrument included a 1525 Binary Pump, a Model 1500 Column Heater and a 2998 Photodiode Array Detector. Because the SEC was performed with a UV detector, the organics detected were UV-responsive substances. In the SEC results, the organic matters with the MW between 300-10000 Da, referred to humic substances [21,36], were separated into three categories: Low MW substances (LMW, 300-1400 Da), medium MW substances (MMW, 1400-4200 Da) and high MW substances (HMW, 4200-10000 Da). Humic substances are known to be rich in aromatic carbon [34], and thus the use of HPSEC with UV detector allows the relative contents of humic substances between samples to be easily compared [35], which helps to investigate the factors causing membrane fouling. The proportion of each category was determined by calculating the individual peak area and the total peak area, and the results were used for subsequent correlation analysis.

2.3. Filtration experiments

A commercial polyamide (PA) nanofiltration membrane (MWCO: 1 kDa, RisingSun Membrane Technology (Beijing) Co., Ltd. China), which represents a state-of-the-art commercial membrane and has been heavily used to evaluate filtration performance and membrane fouling [44]. Filtration tests were performed using a laboratory dead-end filtration unit (UFSC40001, Millipore, USA) with an effective area of 45.34 cm^2 at room temperature. Dead-end filtration was used in this study rather than cross-flow, which is more common in practical membranes application, to emphasize the impact of changing waters and corresponding water quality parameters on fouling mechanisms. The applied pressure was provided by N_2 under a constant value of 4 bar. A digital balance (AX523ZH, OHAUS, USA) connected to a computer automatically recorded the weight of the filtered water in real-time (Figure S2). Two filtration cycles were undertaken, separated by backwashing. The volume of feed water was 50 mL for the first filtration cycle. Then, the fouled membrane was turned upside down and backwashed with 10 mL of deionized (DI) water at a mild pressure of 1 bar. Subsequently, the same volume (50 mL) of feed water was conducted for the second filtration cycle. The variation in normalized flux J/J_0 (J is the time-varying flux, J_0 is the initial membrane flux) with the volume of the filtrate was used to investigate the membrane fouling.

To eliminate the influence of membrane impurities, the membrane specimens were pre-soaked in DI water for at least 24 h, followed by the filtration of 200 mL DI water to remove impurities and stabilize the permeate flux.

2.4. Characterization of cake layer

ATR-FTIR provided the functional group properties of the cake layer on the membrane surface. Water contact angle measurements (WCA, OCA15EC, Dataphysics, Germany) were used to indicate the hydrophilicity of the filter cake layer by using the sessile drop method; membrane samples were cut into strips and mounted on a support; the volume of drop water was 2 μL and recording time was 150 s. Scanning electron microscopy (SEM, QUANTA FEG 250, FEI, USA) was utilized to attain information about the morphology and structure of the filter cake layer on the membrane surface. A solid surface zeta potential analyzer (SurPASS^{TM}

3, Anton Paar, Germany) was used to analyze the surface charge properties of the cake layer through streaming potential measurements. 1 mM KCl was used as the electrolyte to measure the zeta potential under neutral pH.

2.5. Correlation analysis

The correlation between individual water quality parameters (pH, zeta potential, Ca^{2+}, E_{254}/E_{365}, E_{253}/E_{203}, DOC, SUVA, humics, biopolymer and the proportion of different molecular weight and fluorescent components in organic matters) and membrane fouling (total fouling, reversible fouling and irreversible fouling) were analyzed using Spearman correlation and the results were presented in a heat map. The correlation analysis was performed in analysis software (OriginPro 2021 USA) with the help of a functional module (correlation plot). The significant differences were considered at $P < 0.05$.

3. Results and discussion

3.1. Properties of raw waters

The raw water properties are shown in Figures 1a-d. The pH value of YWR water was weakly acidic (pH 6.35), perhaps due to the prevailing soil type and acid rain, while the other water samples were weakly alkaline (range from 7.51-7.80). The turbidity of the six waters ranged from 0.0003-0.03 and was in the order of YWR < JM < HZ < NCH < YWV < ZZY, corresponding to reservoir water < river water < lake water as expected (Figure 1a). The zeta potential data showed that all waters were negatively charged, while the lake water had the lowest zeta potential (-17.2 and -12.8 mV for YWV and ZZY, respectively). However, the reservoir water showed the highest zeta potential (-11.6 and -9.8 mV for YWR and JM, respectively) in both regions (Figure 1b). The molecular size of the NOM was analyzed by E_{254}/E_{365}, as shown in Figure 1c. Lake water showed the highest molecular size (low E_{254}/E_{365} value) and the reservoir waters exhibited the lowest molecular size in both regions. ICP-OES analysis was performed to investigate the concentration of different metal ions in the various surface waters (Figure 1d). The dominant metal ions in six waters were Ca^{2+}, Mg^{2+} and Na^{+}, especially for Ca^{2+}, the concentrations of which in the JM, ZZY and NCH waters were higher

than 26 mg/L, while less than 3 mg/L in YWR and HZ waters.

DOC, SUVA (the ratio of UV_{254} to DOC) and FTIR analyses were performed to further elucidate the NOM characteristics. Figure 2a showed that YWR and HZ waters had the lowest DOC concentration (0.95 and 1.21 mg/L, respectively). In contrast, the highest DOC (4.43 mg/L) was found in ZZY water, which was ~4.7 times higher than the YWR water. JM, NCH and YWV waters had moderate DOC concentrations with the value of 2.54, 3.42 and 3.36 mg/L, respectively. Overall, the DOC concentrations of the six different waters followed the order: lake water > river water > reservoir water. The aromatic/hydrophobic content of organic matter in the different water samples was analyzed by SUVA. YWR and HZ waters had the highest SUVA values of 2.69 and 2.65 L/(m·mg), respectively (Figure 2b), indicating a higher proportion of hydrophobic NOM. The SUVA of the other waters ranged from 1.11-1.46 L/(m·mg), indicating more hydrophilic NOM. The chemical functionality of the organic matter was examined by using FTIR (Figure 2c). All waters had strong peaks at wavenumbers of 3392 cm^{-1}, 1638 cm^{-1} and 1114 cm^{-1}. Corresponding to the stretching vibration of O-H or N-H, C=O and C-O-C, respectively [45-47]. Moreover, differences between these waters can also be observed. The intensities of peaks at 2921 cm^{-1} and 2850 cm^{-1} in YWR and HZ waters were slightly higher than other waters. These two peaks relate to the stretching vibration of C-H [48]. Yamamura et al. [25] also found that the intensity of these two peaks was higher in hydrophobic fractions of organic matter across drinking water sources. These findings were consistent with the SUVA data, indicating a higher proportion of hydrophobic NOM in the YWR and HZ waters. The hydrophilicity of the NOM can also be seen by the intensity of the hydroxyl peak in the FTIR spectrum. It was evident that the intensity of hydroxyl groups in YWV, JM, NCH and ZZY waters was generally higher than that in the YWR and HZ waters, indicating that the NOM in these waters was more hydrophilic. These results agree well with the features of SUVA also.

SEC was conducted to analyze the apparent MW distribution (Figure 2d). Four major absorbance peaks in the range of 300-10000 Da were observed in all waters. These peaks are believed to correspond to humic substances (such as humic and fulvic acids) with a high UV

response [49]. The areas of these peaks in the NCH and ZZY waters were significantly higher compared with other waters, indicating the presence of more humic substances in both waters. A weak peak at 30-80 kDa can be attributed to biopolymers (mainly polysaccharides and proteins with double bonds or aromatic structures) with a low UV response [36], which followed the order of YWV > JM > NCH > ZZY > HZ ≈ YWR. To further analyze the compositional characteristics of organic matters, the humic substances were divided into LMW (300-1400 Da), MMW (1400-4200 Da) and HMW (4200-10000 Da) categories according to the position of the peak, and the proportion of each categories were calculated as shown in Table 1. The proportion of LMW component in six waters was similar (~11%). HMW component account for 39% and 29% in YWR and HZ waters, respectively, followed by ZZY (26%) and NCH (24%) waters. While the proportion was only 20% for YWV and 15% for JM water. For MMW component, the proportion in the six waters was opposite to that of HMW component and in the order: YWR < HZ < ZZY < NCH < YWV < JM.

The EEM spectra showed that the intensity of fluorescent organics in YWR, HZ and JM waters was relatively weak (Figures 3a-b and d), indicating the low organics contents, and the dominant fraction of NOM were protein-like and fulvic acid-like substances. For YWV water, protein-like substances were the main component, while the soluble microbial by-product (SMP) -like and fulvic-acid like substances were also clearly visible (Figure 3c). The fractions of the NOM in NCH and ZZY waters were similar and markedly different from the above four waters. Specifically, the fluorescent intensity of humic-like and fulvic-like substances in NCH and ZZY waters were far higher than other waters and consistent with the SEC results. While the fluorescence intensity of the protein-like and SMP-like substances was also stronger (Figures 3e-f). Further, the fluorescence regional integration (FRI) was applied to quantify the proportion of each fluorescence component (Figure S4). The proportion of protein-like (average: ~56%) was significantly higher than that of humic-like substances (average: ~30%) in YWR, YWV, NCH and ZZY waters, however, the proportion of these two components in HZ and JM waters were found similar (~41%).

3.2. NF performance for various surface waters

The rate of normalized flux decline as a function of filtrate volume was in the order of HZ < YWR < ZZY < NCH < JM < YWV (Figure 4a), thus HZ and YWV waters caused the least and greatest membrane fouling, respectively. The flux of HZ and YWR waters decreased to 95.2% and 94.7% of their initial values, respectively after the first filtration cycle. After backwashing, both waters exhibited a complete flux recovery (J_b/J_0, where J_b and J_0 are the flux after backwashing and initially value), indicating the reversible fouling. Unexpectedly, NCH and ZZY waters, which had the highest DOC concentrations and high amounts of Ca^{2+} caused only moderate membrane fouling. In contrast, JM water, which had a lower DOC concentration, and the YWV water with a similar DOC concentration and lower Ca^{2+} concentration than NCH water, showed greater membrane fouling. In addition, YWV, JM, NCH and ZZY waters caused irreversible fouling. The flux recovery after the first filtration cycle for the above four waters was 94.6%, 98.4%, 99.7% and 99.1%, respectively. The corresponding proportions of reversible and irreversible fouling were calculated as shown in Table 2. It was worth pointing out that this study investigated NF membrane fouling primarily in a bench-scale and we focused on the membrane fouling pattern/difference caused by different surface waters rather than the fouling degree. Thus, we performed a relative low filtration volume (50 mL per cycle), as this filtration method was commonly used to assess NF membrane fouling at laboratory scale [35]. Although prolonging the filtration time will more practical to investigate membrane fouling, it has shown the difference of membrane fouling between different surface waters after 50 mL filtration. The flux decline results indicated the characteristics and quality of NOM, rather than its quantity, is more important for membrane fouling. Further, the combination of high Ca^{2+} and DOC concentrations did not cause a synergistic enhancement of membrane fouling. Thus, additional analysis was required to explore the potential fouling mechanism.

The separation mechanism of NF membranes includes size exclusion, Donnan effect and dielectric exclusion [50]. Among these separation mechanisms, Donnan effect and dielectric exclusion are considered to play an important role in ion separation. However, in this study, we

focused on the separation of NOM in surface waters, which has a relatively large molecular weight, mainly over 1000 Da. Thus, the dominant separation mechanism is considered to be the size exclusion. The performance of the NF membrane in removing organic matter was investigated by SEC (Figures 4b-c). The intensity of all peaks decreased substantially after filtration (Figure 4b). Especially for the biopolymers (30-80 kDa), the corresponding peak intensity of the filtrate was almost indistinguishable from the baseline, thus the membrane achieved a complete removal of biopolymers. However, the removal of humic substances was less than expected based on the membrane's MW cut-off (1 kDa). Figure 4c shows the rejection rate of humic substances based on the SEC peak area. As can be seen that the removal efficiency of the membrane for the six waters was less than 44%, and as low as 20% for the ZZY water, indicating that most humic substances passed through the membrane. In comparison, a higher removal from 38%-43% was observed in YWR, HZ and YWV waters. For YWR and HZ waters, the high rejection can be attributed to more hydrophobic compounds present in both waters (Figure 2b). According to a previous study, the relatively hydrophilic membrane has a greater rejection of hydrophobic and aromatic substances than hydrophilic matters [51]. Although the YWV water had significantly lower hydrophobicity than the YWR and HZ waters, there were a large amount of biopolymers present. It is accepted that high MW biopolymers will adsorb on the membrane surface and block the membrane pores during filtration, thus improving the rejection of low MW humic substances [52]. In comparison, NCH and ZZY waters had a relatively large amount of fulvic acid-like substances. They tended to pass through the membrane more easily owing to their small size and relatively weak interfacial interactions with the membrane. The rejection of different components in humic substances was analyzed as shown in Figure 4d. For the HMW component, the rejection for YWR, HZ and YWV waters was 49%, 54% and 55%, respectively, which was significantly higher than that of JM, NCH and ZZY waters (25%, 34% and 20%, respectively.). In addition, for MMW and LMW components, the membrane also exhibited an improved rejection for YWR, HZ and YWV waters. These results further indicated that the higher hydrophobicity of NOM contributes to higher rejection and the deposition of the high MW component on the membrane surface

improved the rejection of low MW substances. It is worth noting that although the MW of humic substances, especially for HMW (4200-10000 Da) and MMW (1400-4200 Da) components, are over the MW cut-off of the membrane (1000 Da), the membrane showed poor rejection. This can be explained as follows: on the one hand, the MW of humic substances calculated from SEC is mainly based on their hydraulic volume (retention time in the gel). However, although humic substances are rich in aromatic carbon, they are not entirely composed of a rigid aromatic skeleton and their structure also contain some aliphatic linkages, side chains and oxygen-containing groups [34]. Therefore, they have a flexible structure in surface waters [53]. During NF operation, the spatial structure of humic substances tend to be compressed under high pressure, which makes them permeate through the membrane more easily. On the other hand, the MW cut-off of the membrane is defined by the rejection of specific organic molecules (90% rejection by the membrane), such as polyethylene glycol [54]. However, the rejection of the membrane is also affected by molecular configuration, hydrophilicity, etc., which means that rejection can differ for molecules with distinct spatial structure and chemical properties, even if they have the same molecular weight. The rejection performance of organic matter was also evaluated by EEM (Figures S5-6). Compared with the feed water, humic substances in filtrate showed a relatively high level, again emphasizing the unfavorable rejection of humic substances.

The backwash water was also analyzed by SEC and EEM to provide further insights into the rejection performance of the membrane. Figure S7 showed that the peak areas of biopolymers in six backwash waters were higher, demonstrating that most biopolymers were rejected and accumulated on the membrane surface. As for humic substances, YWV water showed the highest peak area in all backwash waters, and its value was ~1.4 times that of ZZY water. However, its peak area in the feed water was not the highest among all feed waters, which was only 54% of ZZY water. This further indicated that the deposited biopolymers increased the rejection of humic substances.

3.3. Characteristics of the fouled membranes

Membrane fouling is mainly caused by the adsorption, pore blocking and cake layer

formation of particulate and organics in the membrane (as shown in Figure 5a) [3]. Measurements of the water contact angle, FTIR spectra and surface zeta potential of the membrane fouled by different surface waters were performed to reveal the fouling degree and the properties of the cake layer on the membrane surface. Figure 5b showed the variation of contact angle over time. Compared with the virgin PA membrane, the contact angles of the membranes decreased after being fouled by surface waters. The contact angle of the membrane fouled by JM and YWV waters decreased rapidly over the first 15 s. NCH and ZZY waters had a moderate decline, while the shape of the YWR and HZ waters plots was basically consistent with the virgin PA membrane. These data support the findings that the JM and YWR waters caused greater membrane fouling, as shown by flux decline results. The results of FTIR showed that the intensity of the hydroxyl peak was greater for the fouled membranes than the virgin membrane, especially for YWV, JM and NCH waters (Figure 5c). The retained NOM is the principal contribution to the increase of hydroxyl peak intensity and these results illustrated that more NOM in YWV, JM and NCH waters deposited on the membrane surface. The surface zeta potential of the fouled membranes reveals the charge properties of the cake layer (Figure 5d). The virgin membrane exhibited a negative charge of -66.89 mV, and after filtration of the surface waters, the zeta potential of fouled membranes all increased slightly (became less negative). The membrane fouled by YWV water showed the highest (less negative) zeta potential value compared to the other waters. This is explained by the deposited NOM being less negatively charged than the virgin membrane. During filtration, the ionized groups on the membrane surface are coated by weakly ionized or non-ionized NOM, resulting in increased zeta potential [55].

The flux decline and the characteristics of the fouled membrane illustrated the fouling degree of the membrane in different waters. Combined with the result of the water quality analysis in Section 3.1, these findings led us to consider how these characteristics affect membrane fouling and whether there is a relationship exists between specific water quality parameters (i.e. biopolymer, DOC) and membrane fouling.

3.4. Discussion: mechanisms of membrane fouling

The analysis demonstrated that DOC or Ca^{2+} contents were not the main causes of membrane fouling. Moreover, DOC and Ca^{2+} did not show a synergistic enhancement effect on membrane fouling. These findings suggest that for surface waters, the quality and chemistry rather than the amount of NOM are more important for membrane fouling. To identify the dominant factor causing membrane fouling and explore whether there is a correlation between specific water quality parameters (i.e. pH, Ca^{2+}, DOC, biopolymer, etc.) and membrane fouling, a correlation analysis was established (Figure 6). The degree of membrane fouling ($1-(J_{50}/J_0)$, where J_{50} and J_0 are the flux after 50 mL and initially, respectively) strongly correlates to the biopolymer contents (R = 0.94, P < 0.05). This correlation is very strong, considering the diversity of the six surface waters examined. These results demonstrated that biopolymer content was the principal cause of membrane fouling and can be used as a universal indicator of membrane fouling across a range of surface waters. To the best of our knowledge, this is the first study of NF membrane fouling using a series of surface waters (six waters) with significant differences in source and characteristics, and a significant correlation between biopolymer content and membrane fouling was found. In addition, the proportion of MMW component in humic substances (%-MMW) also exhibited a positive correlation with membrane fouling (R = 0.89, P < 0.05). Biopolymers are effectively sticky bio-macromolecules. During NF operation, these viscous substances can agglomerate inorganic and organic molecules, forming a compact gel layer adhered tightly to the membrane surface, which blocks the effective water channels and causes severe membrane fouling [56]. For MMW, although their MW is over the MW cut-off of the membrane, considering the flexible structure of humic substances and the compression of their spatial structure during NF operation, their operational size probably approaches the NF membrane pores, thus causing blockage of the membrane and flux decline. However, the proportion of HMW component in humic substances (%-HMW) showed an unexpectedly negative correlation with membrane fouling (R = -0.89, P < 0.05). This is an interesting finding that indicates a higher proportion of HMW in humic substances may have a protective effect on the membrane. A reasonable explanation for this protective effect is that

404 the HMW component is preferentially deposited on the membrane surface, forming a
405 'controlling layer' that prevents the low MW organic matters from entering and blocking the
406 membrane pore. A similar protective mechanism has previously been reported in the literature
407 [57]. For all other factors (such as Ca^{2+}, DOC, zeta potential, humic substances content, etc.),
408 the *P* values > 0.05, indicating no significant correlation with these factors on an individual
409 basis. As for the type of fouling is concerned, biopolymer content and irreversible fouling were
410 found positively correlated ($R = 0.93$, $P < 0.05$), indicating that these viscous macromolecules
411 tightly adhered to the membrane surface, which were unable to be removed completely by
412 backwashing. The type of membrane fouling also correlates to the chemistry and molecular
413 composition properties of the organic matters. SUVA was found to be positively correlated with
414 reversible fouling ($R = 0.81$, $P < 0.05$), and this is mainly due to the weak adhesion between
415 hydrophobic organic matters and the hydrophilic membrane. %-MMW and %-HMW were
416 negatively and positively correlated with reversible fouling, respectively ($R = -0.87$, $P < 0.05$
417 and $R = 0.87$, $P < 0.05$), suggesting that more %-HMW is beneficial for reducing irreversible
418 fouling.

419 In previous studies, Ca^{2+} played a crucial role in UF and NF membrane fouling, as it can
420 act as a bridge between negatively charged NOM and the membrane, forming a denser cake
421 layer which causes significant flux decline [28,58]. However, in the present study, Ca^{2+} showed
422 little correlation with membrane fouling ($R = 0.6$, $P > 0.05$). This discrepancy can be explained
423 by the different characteristics between model humic substances and natural humic substances.
424 Most previous studies used commercial humic acid as a model substance when investigating
425 the effect of Ca^{2+} on membrane fouling. However, commercial humic acid exhibits differences
426 from natural humic substances, including composition, hydrophilicity and molecular weight
427 [34,35]. Thus, natural humic substances can interact with Ca^{2+} differently compared to
428 commercial humic acid. For example, previous research found a noticeable influence of Ca^{2+}
429 on membrane fouling with commercial humic acid, but not with a natural humic substance.
430 Further analysis found that the commercial humic acid, with higher hydrophobicity, aggregated
431 in the presence of Ca^{2+}, while the natural humic substance did not [59]. Therefore, in the

presence of Ca^{2+}, the commercial humic acid is more prone to form a dense cake layer, leading to severe membrane fouling. Conversely, natural humic substances probably form a looser structure, due to weaker interaction with Ca^{2+}, thus producing less membrane fouling. A similar phenomenon that Ca^{2+} has little effect on membrane fouling when using natural waters has been found in previous studies [25,39,60].

Humic substances have also been identified as the main cause of NF membrane fouling in previous work [22,37]. However, in this study, no significant correlation existed between humic substances content and membrane fouling (R = 0.31, P > 0.05). Humic substances are recognized as hydrophobic NOM components relative to proteins and polysaccharides [61]. Thus, the weak correlation between humic substances and membrane fouling could be attributed to the fact that hydrophilic NOM was mainly responsible for membrane fouling [25]. Although there was no significant correlation between the content of humic substances and membrane fouling, the MW composition of humic substances was strongly related to membrane fouling. These findings further highlighted the compositional characteristics and quality of humic substances, rather than their quantity, are more important for evaluating membrane fouling.

The results of this study found that high biopolymer content was the principal cause of NF membrane fouling and irreversible fouling, while HMW had a positive effect on NF membrane fouling prevention. Therefore, this study highlights the importance of biopolymers. High biopolymer content caused severe membrane fouling, especially irreversible fouling, thus reducing biopolymer contents by effective pretreatment may improve NF sustainable performance. From the perspective of the membrane, anti-fouling surface construction, such as hydrophilic or super-hydrophilic modifications could prevent NOM from attaching to the membrane surface and alleviate membrane fouling. In addition, the hydrophobicity of NOM was positively correlated with reversible fouling, which means that hydrophobic NOM was easier to be removed from the membrane by hydraulic cleaning. Therefore, enhancing the sheer force of the water flow on the membrane surface, such as improving the flow velocity under cross-flow operation, could help reduce the adhesion of hydrophobic NOM to the membrane

and optimize permeate performance. Moreover, specific attention also should be focused on the protective role of HMW and the aggravated fouling of MMW component. Oxidative pretreatment may exacerbate subsequent NF fouling due to the disintegration of HMW into MMW and LMW. Finally, more efforts are needed to identify the positive or negative role of specific NOM components in the NF process, to develop more efficient and sustainable NF technologies.

4. Conclusions

This study systematically investigated the water quality characteristics of six representative surface waters and their NF performance and fouling potential. The key contributions to the knowledge of the study are summarized as follows:

1. Biopolymers in surface waters were completely removed by the NF membrane, while the removal of humic substances (< 42%) was less than expected based on the membrane's MW cut-off. The hydrophobicity of NOM was correlated to higher rejection and reversible fouling.
2. Biopolymer content was found to predict NF fouling behaviors by surface waters. Conversely, Ca^{2+} and humic substances contents could not explain the membrane fouling observed.
3. The HMW component in humic substances reduced NF membrane fouling. This positive effect can be explained by the HMW component preferentially depositing on the membrane surface, forming a controlling layer that prevents low MW organics from entering and blocking the membrane pores.

Appendix A. Supporting Information

Supporting Information contains eleven figures and one table that complement the results summarized in the paper. These are the correlation coefficient and significance between

individual water quality parameters and membrane fouling (**Table S1**); sampling location of raw water (**Figure S1**); schematic of the filtration setup (**Figure S2**); conductivity of six waters and aromatic ring substitution degree of NOM (**Figure S3**); fluorescence regional integration of EEM spectrum (**Figure S4**); EEM fluorescence spectra of different surface waters after nanofiltration (**Figure S5**); the rejection of organic matters as indicated by EEM fluorescence intensity (**Figure S6**); Molecular weight distribution of different backwash waters (**Figure S7**); EEM fluorescence spectra of different backwash waters (**Figure S8**); SEM images of the virgin and fouled membranes (**Figures S9-10**); Spearman correlation between individual water quality parameters and membrane fouling (**Figure S11**).

Author contributions

Long Tian, Ting Liu and Wenzheng Yu designed the experiments; Long Tian completed the main experiments and prepared the draft manuscript; Peng Zhou was involved in some of the experiments and data analysis; Zhaoyang Su, Ting Liu, Nigel Graham, Tom Bond and Wenzheng Yu helped to discuss the results and revise the manuscript; Ting Liu and Wenzheng Yu made the final revision to the manuscript.

Declaration of competing interest

The authors declare that they have no known competing financial interests or personal relationships that may have influenced the work reported in this paper.

Acknowledgements

This work was financially supported by the Key Research and Development Plan of the Ministry of Science and Technology (2019YFC1906501 and 2019YFD1100104), the National Natural Science Foundation of China (No. 42107224), and the Beijing Natural Science Foundation (No. JQ21032). It was also supported by the UK Engineering and Physical Sciences

Research Council (grant number EP/N010124/1). The authors would also like to thank Muhammad Saboor Siddique for his help with the revision of the paper.

References

[1] T.E. Culp, B. Khara, K.P. Brickey, M. Geitner, T.J. Zimudzi, J.D. Wilbur, S.D. Jons, A. Roy, M. Paul, B. Ganapathysubramanian, Nanoscale control of internal inhomogeneity enhances water transport in desalination membranes, Science 371 (6524) (2021) 72-75, https://doi.org/10.1126/science.abb8518.

[2] Y. Yao, P. Zhang, C. Jiang, R.M. DuChanois, X. Zhang, M. Elimelech, High performance polyester reverse osmosis desalination membrane with chlorine resistance, Nat. Sustain. 4 (2) (2021) 138-146, https://doi.org/10.1038/s41893-020-00619-w.

[3] R. Zhang, Y. Liu, M. He, Y. Su, X. Zhao, M. Elimelech, Z. Jiang, Antifouling membranes for sustainable water purification: strategies and mechanisms, Chem. Soc. Rev. 45 (21) (2016) 5888-5924, https://doi.org/10.1039/C5CS00579E.

[4] J. Liu, W. Yang, Water sustainability for China and beyond, Science 337 (6095) (2012) 649-650, https://doi.org/10.1126/science.1219471.

[5] T. Tao, K. Xin, Public health: A sustainable plan for China's drinking water, Nature. 511 (7511) (2014) 527-528, https://doi.org/10.1038/511527a.

[6] K. Plakas, A. Mantza, S. Sklari, V. Zaspalis, A. Karabelas, Heterogeneous Fenton-like oxidation of pharmaceutical diclofenac by a catalytic iron-oxide ceramic microfiltration membrane, Chem. Eng. J. 373 (2019) 700-708, https://doi.org/10.1016/j.cej.2019.05.092.

[7] Y. Huang, X. Feng, Polymer-enhanced ultrafiltration: Fundamentals, applications and recent developments, J. Memb. Sci. 586 (2019) 53-83, https://doi.org/10.1016/j.memsci.2019.05.037.

[8] Y.-Z. Wu, H.-X. Li, Z.-L. Xu, P. Li, Z.-M. Zhan, P.-P. Li, S.-J. Xu, Ceramic hollow fiber NF membrane incorporating UiO-66 for the chlorinated hydrocarbons removal, Chem. Eng. J. 435 (2022) 134789, https://doi.org/10.1016/j.cej.2022.134789.

[9] V. Albergamo, B. Blankert, E.R. Cornelissen, B. Hofs, W.-J. Knibbe, W. van der Meer, P. de Voogt, Removal of polar organic micropollutants by pilot-scale reverse osmosis drinking

542 water treatment, Water Res. 148 (2019) 535-545,
543 https://doi.org/10.1016/j.watres.2018.09.029.
544 [10] J. Xu, T.N. Tran, H. Lin, N. Dai, Removal of disinfection byproducts in forward osmosis
545 for wastewater recycling, J. Memb. Sci. 564 (2018) 352-360,
546 https://doi.org/10.1016/j.memsci.2018.07.041.
547 [11] B. Van der Bruggen, C. Vandecasteele, Flux decline during nanofiltration of organic
548 components in aqueous solution, Environ. Sci. Technol. 35 (17) (2001) 3535-3540,
549 https://doi.org/10.1021/es0100064.
550 [12] A. Lee, J.W. Elam, S.B. Darling, Membrane materials for water purification: design,
551 development, and application, Environ. Sci.: Water Res. Technol. 2 (1) (2016) 17-42,
552 https://doi.org/10.1039/C5EW00159E.
553 [13] R. Das, T. Lindström, P.R. Sharma, K. Chi, B.S. Hsiao, Nanocellulose for Sustainable
554 Water Purification, Chem. Rev. 122 (9) (2022) 8936-9031,
555 https://doi.org/10.1021/acs.chemrev.1c00683.
556 [14] D. Li, W. Lin, R. Shao, Y.-X. Shen, X. Zhu, X. Huang, Interaction between humic acid
557 and silica in reverse osmosis membrane fouling process: A spectroscopic and molecular
558 dynamics insight, Water Res. 206 (2021) 117773,
559 https://doi.org/10.1016/j.watres.2021.117773.
560 [15] S.P. Sambo, S.S. Marais, T.A. Msagati, B.B. Mamba, T.T. Nkambule, Quantification of
561 biodegradable natural organic matter (NOM) fractions and its impact on bacterial
562 regrowth in a South African Water Treatment Plant, J. Water Process Eng. 36 (2020)
563 101332, https://doi.org/10.1016/j.jwpe.2020.101332.
564 [16] W. Chen, H.-Q. Yu, Advances in the characterization and monitoring of natural organic
565 matter using spectroscopic approaches, Water Res. 190 (2021) 116759,
566 https://doi.org/10.1016/j.watres.2020.116759.
567 [17] D. Zhang, K. Zhang, K. Chen, Y. Xue, J. Liang, Y. Cai, Mitigation of organic fouling of
568 ultrafiltration membrane by high-temperature crayfish shell biochar: Performance and
569 mechanisms, Sci. Total Environ. 820 (2022) 153183,

https://doi.org/10.1016/j.scitotenv.2022.153183.

[18] L. Bai, H. Wu, J. Ding, A. Ding, X. Zhang, N. Ren, G. Li, H. Liang, Cellulose nanocrystal-blended polyethersulfone membranes for enhanced removal of natural organic matter and alleviation of membrane fouling, Chem. Eng. J. 382 (2020) 122919, https://doi.org/10.1016/j.cej.2019.122919.

[19] J. Guo, X. Zhu, Q. Wang, W. Liu, Y. Wang, The combination effect of preozonation and CNTs layer modification on low-pressure membrane fouling control in treating NOM and EfOM, J. Memb. Sci. 627 (2021) 119225, https://doi.org/10.1016/j.memsci.2021.119225.

[20] A.E. Contreras, Z. Steiner, J. Miao, R. Kasher, Q. Li, Correction to Studying the Role of Common Membrane Surface Functionalities on Adsorption and Cleaning of Organic Foulants Using QCM-D, Environ. Sci. Technol. 45 (15) (2011) 6309-6315, https://doi.org/10.1021/es3009584.

[21] T. Liu, B. Yang, N. Graham, W. Yu, K. Sun, Trivalent metal cation cross-linked graphene oxide membranes for NOM removal in water treatment, J. Memb. Sci. 542 (2017) 31-40, https://doi.org/10.1016/j.memsci.2017.07.061.

[22] L. Shan, H. Fan, H. Guo, S. Ji, G. Zhang, Natural organic matter fouling behaviors on superwetting nanofiltration membranes, Water Res. 93 (2016) 121-132, https://doi.org/10.1016/j.watres.2016.01.054.

[23] J. Shim, S. Park, K.H. Cho, Deep learning model for simulating influence of natural organic matter in nanofiltration, Water Res. 197 (2021) 117070, https://doi.org/10.1016/j.watres.2021.117070.

[24] S. Wu, X. Hua, B. Ma, H. Fan, R. Miao, M. Ulbricht, C. Hu, J. Qu, Three-dimensional analysis of the natural-organic-matter distribution in the cake layer to precisely reveal ultrafiltration fouling mechanisms, Environ. Sci. Technol. 55 (8) (2021) 5442-5452, https://doi.org/10.1021/acs.est.1c00435.

[25] H. Yamamura, K. Okimoto, K. Kimura, Y. Watanabe, Hydrophilic fraction of natural organic matter causing irreversible fouling of microfiltration and ultrafiltration membranes, Water Res. 54 (2014) 123-136, https://doi.org/10.1016/j.watres.2014.01.024.

598 [26] N. Her, G. Amy, J. Chung, J. Yoon, Y. Yoon, Characterizing dissolved organic matter and
599 evaluating associated nanofiltration membrane fouling, Chemosphere. 70 (3) (2008) 495-
600 502, https://doi.org/10.1016/j.chemosphere.2007.06.025.
601 [27] K. Chon, J. Cho, Fouling behavior of dissolved organic matter in nanofiltration
602 membranes from a pilot-scale drinking water treatment plant: an autopsy study, Chem.
603 Eng. J. 295 (2016) 268-277, https://doi.org/10.1016/j.cej.2016.03.057.
604 [28] L.-F. Wang, D.-Q. He, W. Chen, H.-Q. Yu, Probing the roles of Ca^{2+} and Mg^{2+} in humic
605 acids-induced ultrafiltration membrane fouling using an integrated approach, Water Res.
606 81 (2015) 325-332, https://doi.org/10.1016/j.watres.2015.06.009.
607 [29] B. Li, X. He, P. Wang, Q. Liu, W. Qiu, J. Ma, Opposite impacts of K^{+} and Ca^{2+} on
608 membrane fouling by humic acid and cleaning process: evaluation and mechanism
609 investigation, Water Res. 183 (2020) 116006,
610 https://doi.org/10.1016/j.watres.2020.116006.
611 [30] M. Lejars, A. Margaillan, C. Bressy, Fouling release coatings: a nontoxic alternative to
612 biocidal antifouling coatings, Chem. Rev. 112 (8) (2012) 4347-4390,
613 https://doi.org/10.1021/cr200350v.
614 [31] A.E. Childress, M. Elimelech, Effect of solution chemistry on the surface charge of
615 polymeric reverse osmosis and nanofiltration membranes, J. Memb. Sci. 119 (2) (1996)
616 253-268, https://doi.org/10.1016/0376-7388(96)00127-5.
617 [32] G. Mustafa, K. Wyns, A. Buekenhoudt, V. Meynen, New insights into the fouling
618 mechanism of dissolved organic matter applying nanofiltration membranes with a variety
619 of surface chemistries, Water Res. 93 (2016) 195-204,
620 https://doi.org/10.1016/j.watres.2016.02.030.
621 [33] A.S. Al-Amoudi, Factors affecting natural organic matter (NOM) and scaling fouling in
622 NF membranes: A review, Desalination. 259 (1-3) (2010) 1-10,
623 https://doi.org/10.1016/j.desal.2010.04.003.
624 [34] I. Sutzkover-Gutman, D. Hasson, R. Semiat, Humic substances fouling in ultrafiltration
625 processes, Desalination. 261 (3) (2010) 218-231,

626 https://doi.org/10.1016/j.desal.2010.05.008.
627 [35] H. Yang, W. Xue, M. Liu, K. Yu, W. Yu, Carbon doped Fe_3O_4 peroxidase-like nanozyme
628 for mitigating the membrane fouling by NOM at neutral pH, Water Res. 174 (2020)
629 115637, https://doi.org/10.1016/j.watres.2020.115637.
630 [36] Z. Su, W. Yu, T. Liu, X. Li, N.J. Graham, Y. Lu, M.R. Wiesner, Discovery of welcome
631 biopolymers in surface water: improvements in drinking water production, Environ. Sci.
632 Technol. 55 (3) (2021) 2076-2086, https://doi.org/10.1021/acs.est.0c05758.
633 [37] Y. Guo, T.-y. Li, K. Xiao, X.-m. Wang, Y.F. Xie, Key foulants and their interactive effect
634 in organic fouling of nanofiltration membranes, J. Memb. Sci. 610 (2020) 118252,
635 https://doi.org/10.1016/j.memsci.2020.118252.
636 [38] J.-y. Tian, M. Ernst, F. Cui, M. Jekel, Correlations of relevant membrane foulants with UF
637 membrane fouling in different waters, Water Res. 47 (3) (2013) 1218-1228,
638 https://doi.org/10.1016/j.watres.2012.11.043.
639 [39] K. Kimura, K. Tanaka, Y. Watanabe, Microfiltration of different surface waters
640 with/without coagulation: Clear correlations between membrane fouling and hydrophilic
641 biopolymers, Water Res. 49 (2014) 434-443, https://doi.org/10.1016/j.watres.2013.10.030.
642 [40] L.M. Lynch, N.A. Sutfin, T.S. Fegel, C.M. Boot, T.P. Covino, M.D. Wallenstein, River
643 channel connectivity shifts metabolite composition and dissolved organic matter
644 chemistry, Nat. Commun. 10 (1) (2019) 1-11, https://doi.org/10.1038/s41467-019-08406-
645 8.
646 [41] R. Fabris, C.W. Chow, M. Drikas, B. Eikebrokk, Comparison of NOM character in
647 selected Australian and Norwegian drinking waters, Water Res. 42 (15) (2008) 4188-4196,
648 https://doi.org/10.1016/j.watres.2008.06.023.
649 [42] P. Holubar, T. Grudke, A. Moser, B. Strenn, R. Braun, Effects of bacterivorous ciliated
650 protozoans on degradation efficiency of a petrochemical activated sludge process, Water
651 Res. 34 (7) (2000) 2051-2060, https://doi.org/10.1016/S0043-1354(99)00378-4.
652 [43] W. Chen, P. Westerhoff, J.A. Leenheer, K. Booksh, Fluorescence excitation-emission
653 matrix regional integration to quantify spectra for dissolved organic matter, Environ. Sci.

654 Technol. 37 (24) (2003) 5701-5710, https://doi.org/10.1021/es034354c.
655 [44] M.G. Shin, W. Choi, S.-J. Park, S. Jeon, S. Hong, J.-H. Lee, Critical review and
656 comprehensive analysis of trace organic compound (TOrC) removal with polyamide
657 RO/NF membranes: Mechanisms and materials, Chem. Eng. J. 427 (2022) 130957,
658 https://doi.org/10.1016/j.cej.2021.130957.
659 [45] X. Cheng, P. Li, X. Zhu, C. Luo, L. Zheng, C. Hou, D. Wu, H. Liang, Role of different
660 dimensional carbon nanoparticles in catalytic oxidation of organic pollutants and
661 alleviating membrane fouling during ultrafiltration of surface water, Sep. Purif. Technol.
662 270 (2021) 118804, https://doi.org/10.1016/j.seppur.2021.118804.
663 [46] R. Li, X. Wang, J. Liu, Q. Cui, X. Wang, S. Chen, L. Jiang, Relationship between
664 molecular flexibility and emulsifying properties of soy protein isolate-glucose conjugates,
665 J. Agric. Food Chem. 67 (14) (2019) 4089-4097, https://doi.org/10.1021/acs.jafc.8b06713.
666 [47] T. Liu, H. Zhou, N. Graham, W. Yu, K. Sun, 2D kaolin ultrafiltration membrane with
667 ultrahigh flux for water purification, Water Res. 156 (2019) 425-433,
668 https://doi.org/10.1016/j.watres.2019.03.050.
669 [48] J. Tian, C. Wu, H. Yu, S. Gao, G. Li, F. Cui, F. Qu, Applying ultraviolet/persulfate (UV/PS)
670 pre-oxidation for controlling ultrafiltration membrane fouling by natural organic matter
671 (NOM) in surface water, Water Res. 132 (2018) 190-199,
672 https://doi.org/10.1016/j.watres.2018.01.005.
673 [49] L. Zhang, N. Graham, N. Derlon, Y. Tang, M.S. Siddique, L. Xu, W. Yu, Biofouling by
674 ultra-low pressure filtration of surface water: The paramount role of initial available
675 biopolymers, J. Memb. Sci. 640 (2021) 119740,
676 https://doi.org/10.1016/j.memsci.2021.119740.
677 [50] R. Wang, S. Lin, Pore model for nanofiltration: History, theoretical framework, key
678 predictions, limitations, and prospects, J. Memb. Sci. 620 (2021) 118809,
679 https://doi.org/10.1016/j.memsci.2020.118809.
680 [51] W. Yu, T. Liu, J. Crawshaw, T. Liu, N. Graham, Ultrafiltration and nanofiltration
681 membrane fouling by natural organic matter: Mechanisms and mitigation by pre-

682 ozonation and pH, Water Res. 139 (2018) 353-362,
683 https://doi.org/10.1016/j.watres.2018.04.025.
684 [52] D.T. Myat, M.B. Stewart, M. Mergen, O. Zhao, J.D. Orbell, S. Gray, Experimental and
685 computational investigations of the interactions between model organic compounds and
686 subsequent membrane fouling, Water Res. 48 (2014) 108-118,
687 https://doi.org/10.1016/j.watres.2013.09.020.
688 [53] A.S. Koparal, Y.Ş. Yildiz, B. Keskinler, N. Demircioğlu, Effect of initial pH on the removal
689 of humic substances from wastewater by electrocoagulation, Sep. Purif. Technol. 59 (2)
690 (2008) 175-182, https://doi.org/10.1016/j.seppur.2007.06.004.
691 [54] F. Kramer, R. Shang, S. Scherrenberg, L. Rietveld, S. Heijman, Quantifying defects in
692 ceramic tight ultra-and nanofiltration membranes and investigating their robustness, Sep.
693 Purif. Technol. 219 (2019) 159-168, https://doi.org/10.1016/j.seppur.2019.03.019.
694 [55] J. Cho, G. Amy, J. Pellegrino, Y. Yoon, Characterization of clean and natural organic
695 matter (NOM) fouled NF and UF membranes, and foulants characterization, Desalination.
696 118 (1-3) (1998) 101-108, https://doi.org/10.1016/S0011-9164(98)00100-3.
697 [56] S. Peldszus, C. Hallé, R.H. Peiris, M. Hamouda, X. Jin, R.L. Legge, H. Budman, C.
698 Moresoli, P.M. Huck, Reversible and irreversible low-pressure membrane foulants in
699 drinking water treatment: Identification by principal component analysis of fluorescence
700 EEM and mitigation by biofiltration pretreatment, Water Res. 45 (16) (2011) 5161-5170,
701 https://doi.org/10.1016/j.watres.2011.07.022.
702 [57] Q. Song, N. Graham, Y. Tang, M.S. Siddique, K. Kimura, W. Yu, The role of medium
703 molecular weight organics on reducing disinfection by-products and fouling prevention in
704 nanofiltration, Water Res. 215 (2022) 118263,
705 https://doi.org/10.1016/j.watres.2022.118263.
706 [58] Y. Song, X. Li, C. Li, J. Li, Z. Dong, M. Zhang, P. Qi, X. Bai, K. Jiang, Exploring and
707 comparing the roles of Ca^{2+} and Mg^{2+} in small-sized natural organics-induced charged
708 nanofiltration membrane fouling, Sep. Purif. Technol. 251 (2020) 117415,
709 https://doi.org/10.1016/j.seppur.2020.117415.

[59] H. Yamamura, K. Okimoto, K. Kimura, Y. Watanabe, Influence of calcium on the evolution of irreversible fouling in microfiltration/ultrafiltration membranes, J. Water Supply Res. Technol. -AQUA 56 (6-7) (2007) 425-434, https://doi.org/10.2166/aqua.2007.018.

[60] N. Lee, G. Amy, J.-P. Croue, Low-pressure membrane (MF/UF) fouling associated with allochthonous versus autochthonous natural organic matter, Water Res. 40 (12) (2006) 2357-2368, https://doi.org/10.1016/j.watres.2006.04.023.

[61] J.A. Leenheer, Systematic approaches to comprehensive analyses of natural organic matter, Ann. Environ. Sci. 3 (2009) 1-130.

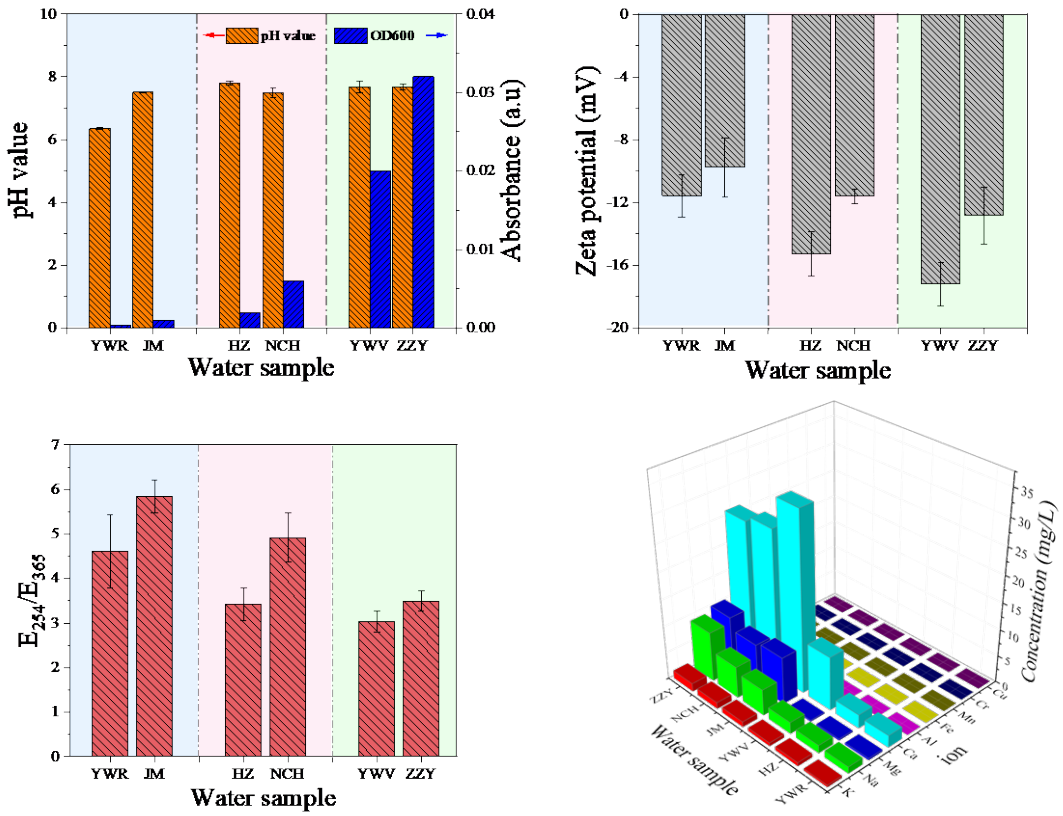


Figure 1. Raw water properties: (a) pH value and turbidity in the form of UV absorption at 600 nm; (b) zeta potential; (c) molecular weight of organic matter, as indicated by the ratio of UV adsorption at 254 to 365 nm; (d) the concentration of various metal ions. The colored rectangles in Figures (a-c) represent different types of water, blue, pink and green represent reservoir waters, river waters and lake waters, respectively, and in each colored rectangle, the left is the southern waters and the right is the northern waters.

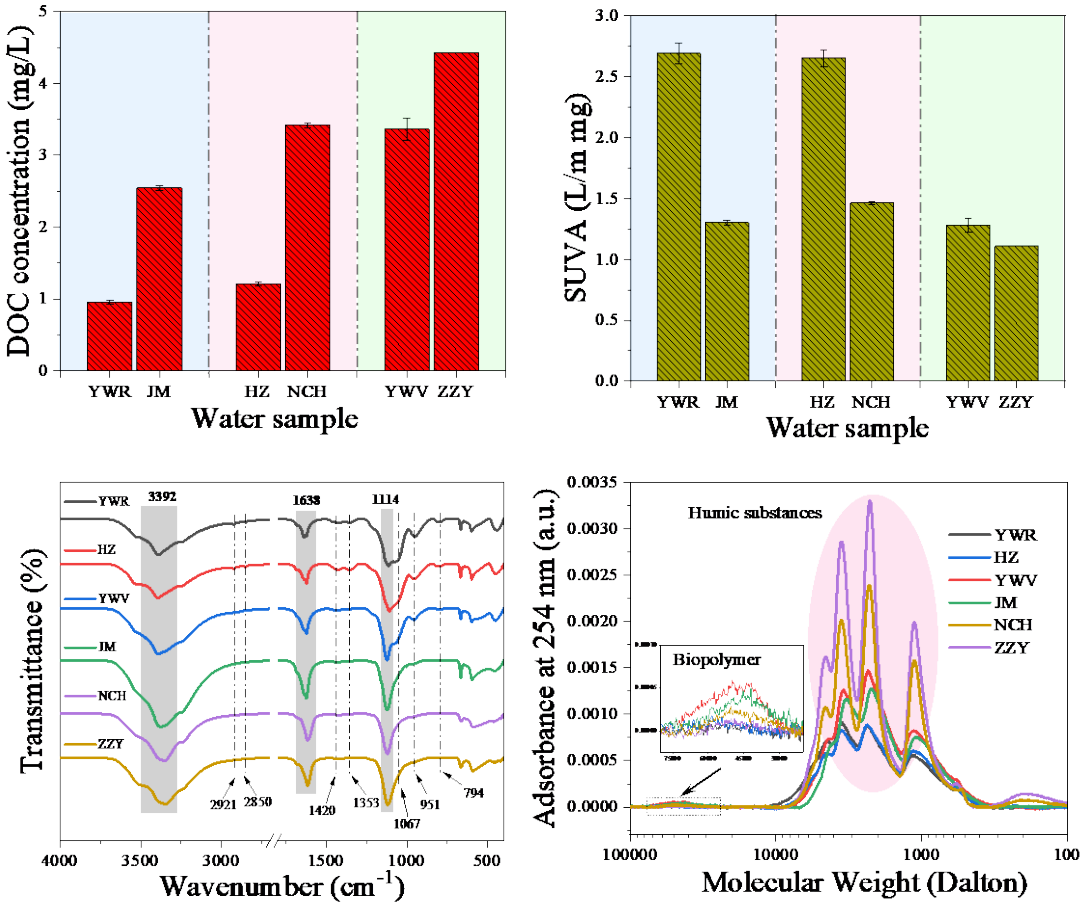


Figure 2. Characteristics of organic matters in different surface waters: (a) DOC concentration; (b) aromaticity as indicated by SUVA value; (c) FTIR spectra (raw water after freeze-drying) and (d) apparent molecular weight distributions. The colored rectangles in Figures a and b represent different types of water, blue, pink and green represent reservoir waters, river waters and lake waters, respectively, and in each colored rectangle, the left is the southern waters and the right is the northern waters.

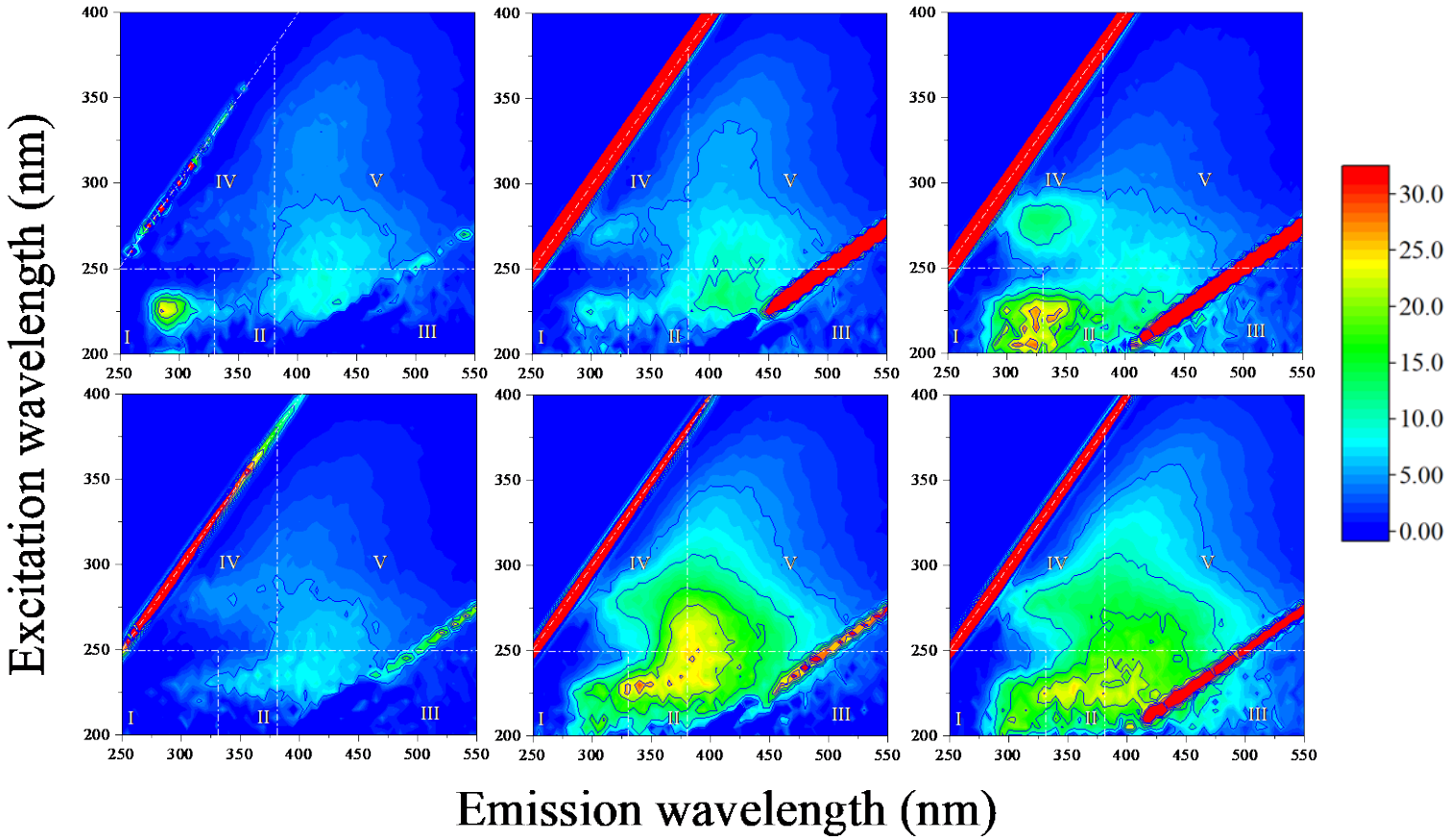


Figure 3. EEM fluorescence spectra of different surface waters. (a) YWR water; (b) HZ water; (c) YWV water; (d) JM water; (e) NCH water and (f) ZZY water, respectively. Region I, II, III, IV and V represent tyrosine-like, tryptophan-like, fulvic acid-like, soluble microbial by-product-like and humic acid-like substances, respectively. Tyrosine-like and tryptophan-like substances are protein-like substances.

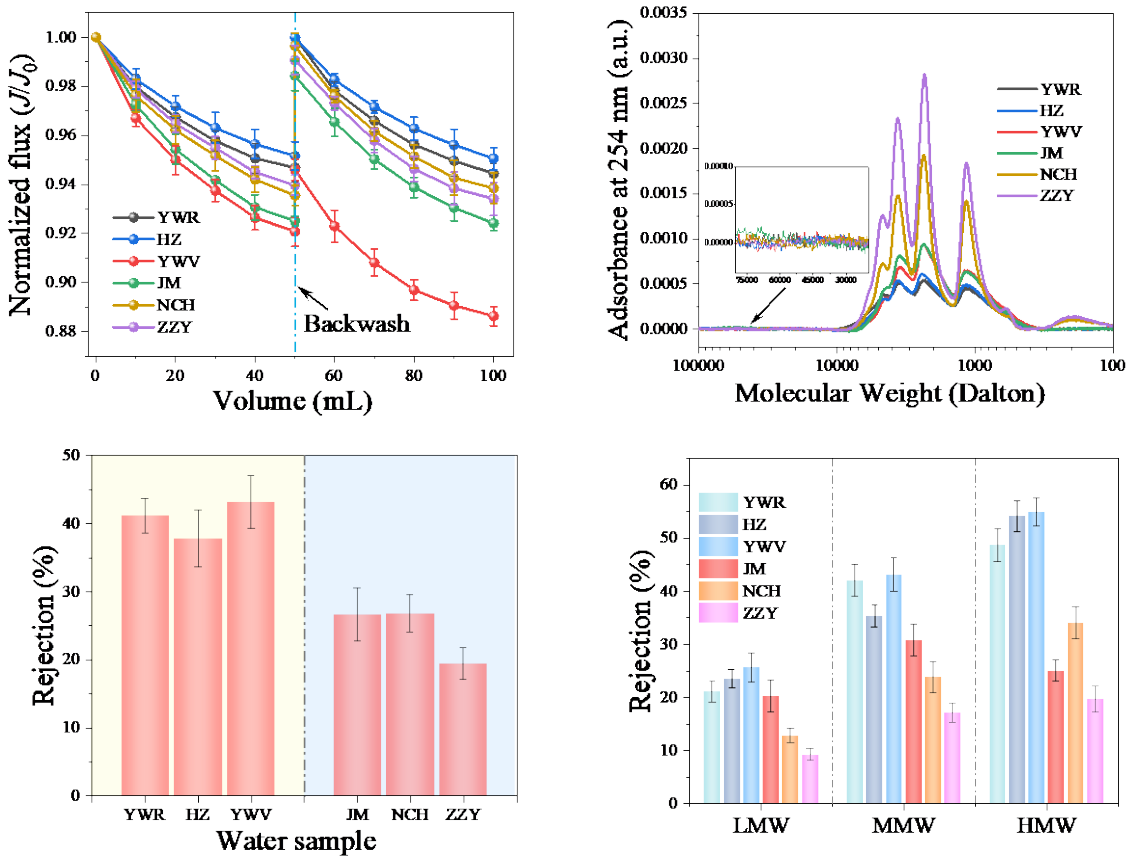


Figure 4. (a) Normalized Flux decline and recovery (after backwashing) with various surface waters for the membrane as a function of permeation volume; (b) molecular weight distribution of organic matters in different surface waters after nanofiltration; (c) the rejection of humic substances in different surface waters, the yellow and blue rectangles represent southern waters and northern waters, respectively; (d) the rejection of LMW, MMW and HMW components in humic substances.

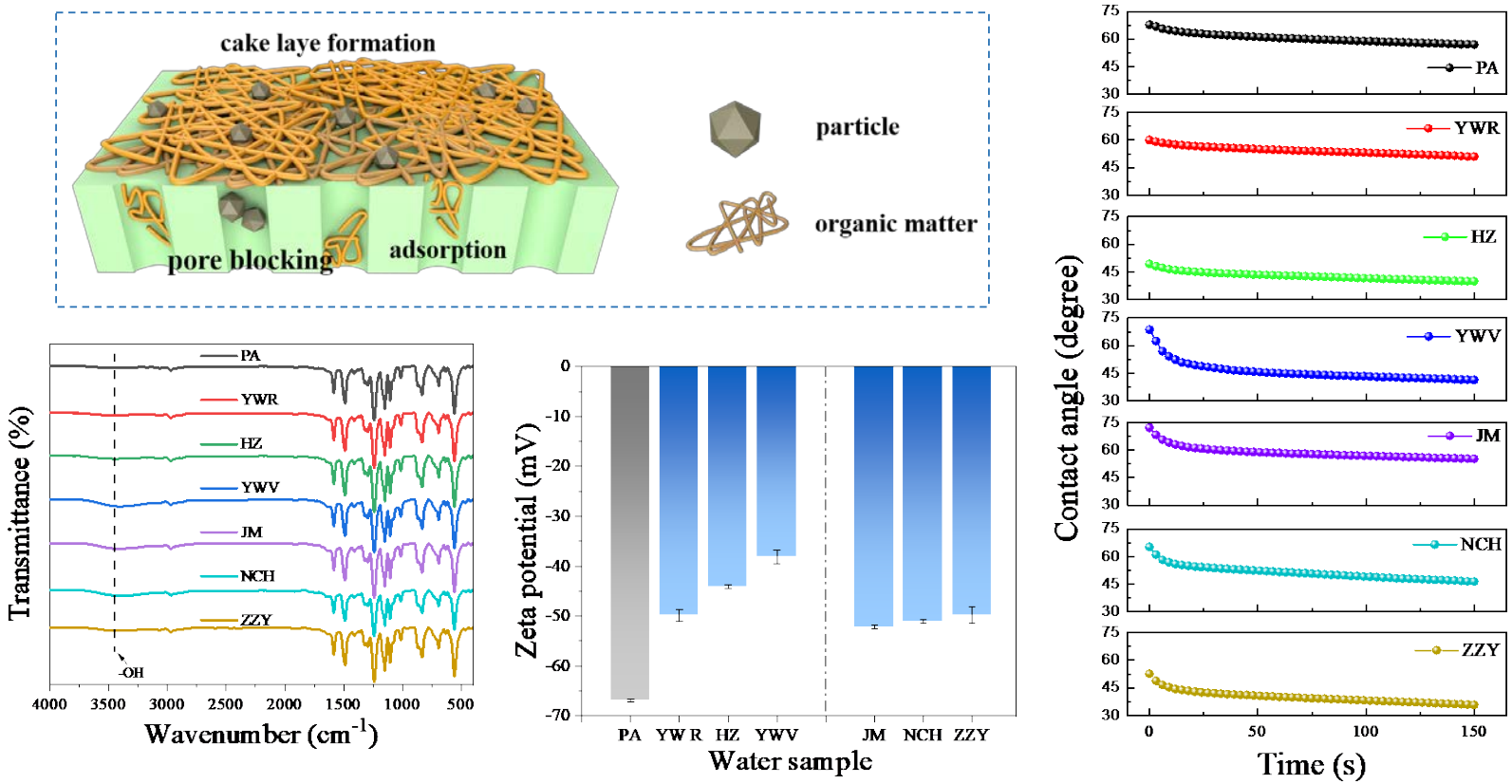


Figure 5. Properties of the membrane fouled by different surface waters: (a) schematic of the three major membrane fouling mechanisms, including pore adsorption, pore blocking and cake layer formation; (b) temporal variation of the water contact angle from 0 to 150 s; (c) ATR-FTIR spectra and (d) surface zeta potential of the fouled membranes.

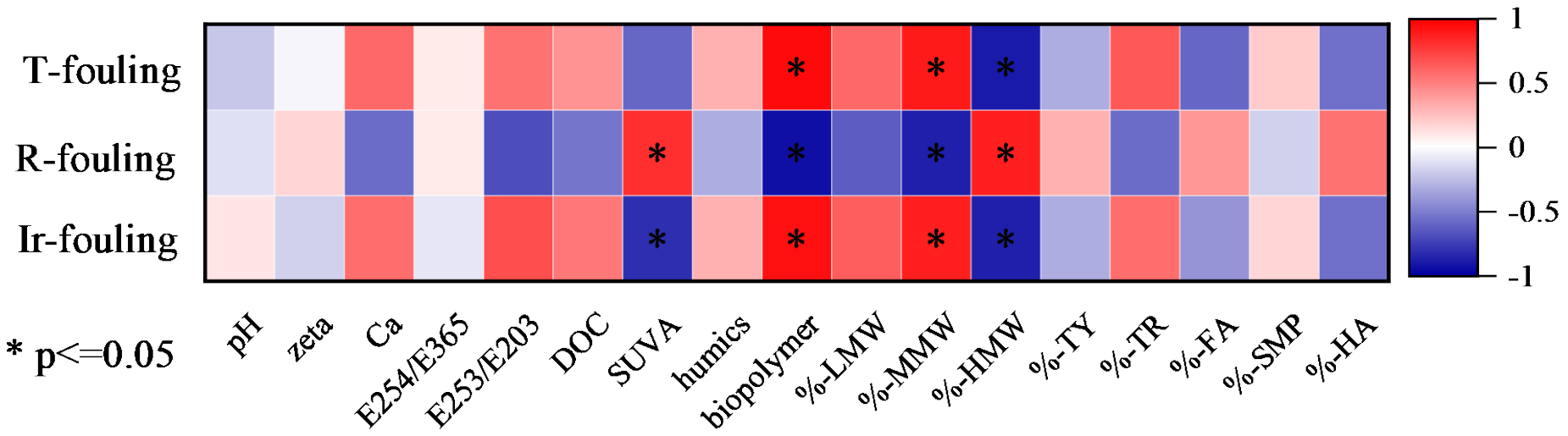


Figure 6. Heat-map of correlations between individual water quality parameters and membrane fouling. The concentration of biopolymer and humic substances were determined by SEC peak area. %-LWM, %-MWM and %-HWM are the proportion of low molecular weight, medium molecular weight and high molecular weight components in humic substances, respectively. %-TY, %-TR, %-FA, %-SMP and %-HA represent the proportion of tyrosine-like, tryptophan-like, fulvic acid-like, soluble microbial by-product-like and humic acid-like fractions in EEM fluorescence spectrum. T-fouling, R-fouling and Ir-fouling are total fouling, reversible fouling and irreversible fouling, respectively. Blue and red indicate a negative and positive correlation, respectively. The symbol * indicates the $P < 0.05$.

Table 1

The proportion of HMW, MMW and LMW components in humic substances.

Water samples	HMW(%)	MMW(%)	LMW(%)
YWR	39	52	9
HZ	29	59	12
YWV	20	68	12
JM	15	72	13
NCH	24	65	11
ZZY	26	64	10

HMW, MMW and LMW represent the high molecular weight, medium molecular weight and low molecular weight.

Table 2

Total fouling, reversible fouling and irreversible fouling of different surface waters.

Water samples	Total fouling (%)	Reversible fouling (%)	Irreversible fouling (%)
YWR	5.3	100	0
HZ	4.8	100	0
YWV	7.9	31.9	68.1
JM	7.5	79.1	20.9
NCH	6.4	94.6	5.4
ZZY	6.0	84.7	15.3